Durability-weighted crediting of blue carbon in coastal industrial symbiosis

TIDE-BC: a tonne-year durability estimator with risk-adjusted issuance for phytoplankton-mediated circular carbon pathways

[1]Saswat Swain [2] Chandrasekhar Panda [3]Pravat Satpathy [4]Sonia Mohapatra

[1,2]Ph.D Scholar, [3,4]R & D Division

[1,2]KSOM - KIIT Deemed to be University ,[3,4]Tekstein Solutions,India

[1]saswat.mck@gmail.com [2]contact@chandrasekarpanda.com [3]pravat@teksteinsolutions.com [4]sonia@teksteinsolutions.com

Abstract—Blue carbon crediting is under scrutiny because prevailing methodologies treat every tonne of fixed carbon as equivalent, irrespective of how long it stays out of the atmosphere. This paper develops TIDE-BC, an accounting framework that discounts fixed carbon by the residence time of the pool it enters, and applies it to a coastal industrial symbiosis loop in which flue gas, nutrient-rich effluent, alkaline steel slag and siliceous ash are routed through a marine microalgal raceway. A coupled model combining depth-averaged photoinhibited growth, cardinal-temperature kinetics, Droop nutrient quotas, seawater carbonate speciation and a closed alkalinity budget is integrated with a durability-equivalence factor derived in closed form as the Laplace transform of an exponential retention kernel. Simulations over six marine species, four process configurations and 512 Sobol draws show that the durability weight of short-cycle biomass products is 0.043, so crediting biomass as permanent overstates removal by 3.8 to 6.1 times. Three of the four configurations are net carbon sources on a grid at 0.71 kg CO_2 kWh^{-1}; the break-even grid intensity is 0.250 kg CO_2 kWh^{-1}. The best configuration delivers 42.8 t CO_2 ha^{-1} yr^{-1} deterministically and a tenth-percentile issuance of 25.0 t CO_2 ha^{-1} yr^{-1}, implying a 30.2% buffer. Two results run against expectation and are reported as such: the diatoms tested fix no carbon at all without a silicate co-feed from ash leachate, and the coccolithophore *Emiliania huxleyi* is a net source at -5.3 t CO_2 ha^{-1} yr^{-1} once calcification is placed on a closed alkalinity budget. The framework is simulation-based and has not been validated against pilot or field data.

Index Terms—Blue carbon, carbon credit durability, circular economy, industrial symbiosis, marine microalgae, ocean alkalinity enhancement, tonne-year accounting.

I. Introduction

The blue economy assigns economic value to the ocean while requiring that the underlying ecosystems remain intact, and blue carbon credits are the principal instrument through which that value is monetised. The instrument is now under pressure. Investigations into forestry and wetland crediting have repeatedly found that issued volumes exceed the removal that can be demonstrated, and the criticism transfers directly to marine projects because the same convention is used: one tonne of carbon fixed is treated as one tonne removed, whatever happens to that carbon afterwards.

The convention is not defensible on physical grounds. Carbon that enters a protein or pigment product is respired within a year or two. Carbon that enters pyrolytic char persists for centuries. Carbon stored as bicarbonate through added alkalinity persists for tens of thousands of years. Treating these as interchangeable is equivalent to valuing a one-year bond and a perpetuity at par. What is missing is not more measurement but an accounting rule that maps residence time onto credit value, and a way of issuing credits that is robust to the fact that residence times are themselves uncertain.

A second gap concerns where the carbon comes from. Most blue carbon projects are conservation projects, which makes additionality contentious. An alternative is to build the sink into industrial infrastructure: coastal steel, cement and thermal power clusters emit concentrated CO_2, discharge nitrogen- and phosphorus-rich effluent that drives coastal eutrophication, and stockpile alkaline slag and siliceous ash. Each of these is a liability. Marine microalgae can convert all four into a single productive stream, and the residues can be routed to pools of very different durability. This is a circular economy problem and a carbon accounting problem at the same time, and the two cannot be solved separately, because the choice of which product to make determines the durability of the carbon.

This paper makes four contributions. First, a durability-equivalence factor is derived in closed form from a retention kernel and a discount rate, giving a single dimensionless weight per storage pool. Second, calcification and engineered alkalinity addition are resolved on one closed budget rather than credited separately, which both removes a double-counting error and reproduces the classical surface-seawater CO_2 release ratio as a derived quantity. Third, a break-even grid carbon intensity is obtained analytically, separating configurations that can ever be creditable from those that cannot. Fourth, credits are issued at a low quantile of the predictive distribution rather than at its mean, which bounds the probability of over-crediting by construction.

The results are not uniformly favourable to the proposed system, and the unfavourable ones are reported in full. Three of the four configurations examined are net carbon sources under present grid conditions. The two diatoms tested produce nothing without a second waste loop supplying silicate. The hypothesis that motivated quantile-based

issuance — that the predictive distribution would be strongly right-skewed — was not supported by the simulations.

II. Background and Related Work

Tonne-year accounting has a long history in forestry, where it was introduced to price temporary storage. It has been criticised for the arbitrariness of the equivalence horizon and for permitting indefinite renewal of short-lived storage. The formulation used here avoids fixing a horizon: instead of asking how many years of storage equal permanence, it discounts the retention function directly, so that the equivalence weight emerges from the residence time and the discount rate alone.

Microalgal CO_2 capture from flue gas is well established at laboratory and pilot scale, and areal productivities in the range of roughly 15 to 30 g dry weight m^{-2} d^{-1} are commonly reported for outdoor marine raceways. Life-cycle assessments of these systems disagree sharply, and the disagreement is traceable to the electricity mix and to whether the biomass is dried. Ocean alkalinity enhancement using steel slag is a younger literature, with the CO_2 uptake per mole of added alkalinity generally placed between 0.7 and 0.85. The microbial carbon pump, which converts a fraction of algal exudate into refractory dissolved organic carbon with millennial residence times, is well documented biogeochemically but has not been incorporated into crediting frameworks.

What has not been done, to the authors' knowledge, is to couple a mechanistic cultivation model to a durability-weighted ledger in which the alkalinity budget, the organic carbon fate partition and the life-cycle emissions are resolved simultaneously, and to propagate parameter uncertainty through to the issued credit volume. That is the object of the present work.

III. System Description

The reference system is a one-hectare open raceway module, 0.25 m deep, co-located with a coastal industrial cluster on the east coast of India. Fig. 1 shows the streams and the fate pools.

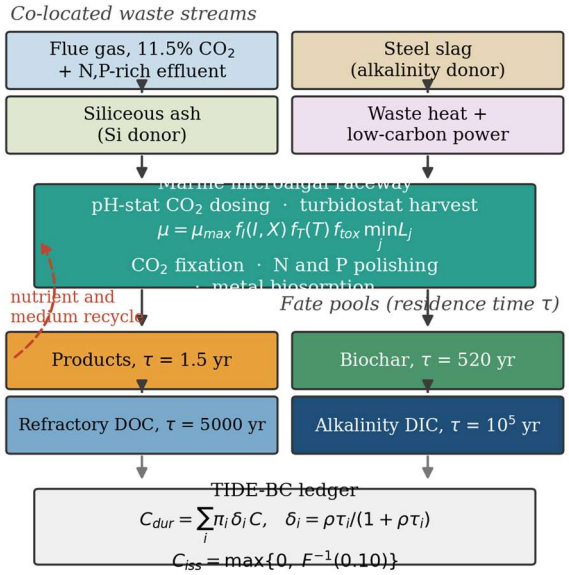

Fig. 1. Industrial symbiosis loop and the TIDE-BC ledger. Four co-located waste streams feed a marine microalgal raceway; fixed carbon is partitioned over four pools whose residence times differ by five orders of magnitude, and each pool is weighted by its durability-equivalence factor before credits are issued at the tenth percentile of the predictive distribution.

Four waste streams enter. Desulphurised flue gas at 11.5% CO_2 is sparged on demand under pH control. Blended industrial and municipal effluent supplies 48 mg N L^{-1} and 6.4 mg P L^{-1} together with 0.85 mg L^{-1} of dissolved metals. Ground steel slag supplies alkalinity. Siliceous ash leachate supplies dissolved silicate, which matters only for diatoms but matters decisively. Waste heat drives hydrothermal carbonisation, which avoids the drying step that dominates the energy balance of dry-route algal processing.

Harvested carbon leaves through four routes. Short-cycle products (protein, pigment, extracellular polymeric substances) return their carbon to the atmosphere within about 1.5 years. Hydrothermal char placed in soil or used as a construction filler is modelled as a two-pool solid with a mean residence time of 520 years. A fraction of the exudate becomes refractory dissolved organic carbon with a residence time of order 5000 years. Alkalinity added to the discharge stores dissolved inorganic carbon on a timescale set by ocean mixing and carbonate compensation, taken as 10^5 years.

IV. Design Methodology

A. Growth kinetics

The specific growth rate combines multiplicative physical and toxicological factors with a Liebig minimum over resource limitations,

$$\mu = \mu_{\max} \cdot f_{\mathrm{I}}(I, X) \cdot f_{\mathrm{T}}(T) \cdot f_{\mathrm{tox}} \cdot \min_{\mathrm{j}} L_{\mathrm{j}} - m(T) \tag{1}$$

where $m(T)$ is maintenance respiration. Irradiance decays with depth through water and biomass self-shading,

$$I(z) = I_0 \exp[-(\sigma X + a_{\mathrm{w}})\, z] \tag{2}$$

and the light factor is the average of an Aiba photoinhibition response over the culture depth, evaluated by 24-point Gauss–Legendre quadrature,

$$f_{\mathrm{I}} = z_{\mathrm{p}}^{-1} \int I / (K_{\mathrm{I}} + I + I^2 / K_{\mathrm{i}})\, \mathrm{d}z \tag{3}$$

Temperature enters through the cardinal temperature model with inflection [8], with $\Delta(T)$ as defined there and the result clipped to the unit interval,

$$f_T = (T - T_{max})(T - T_{min})^2 / \Delta(T) \tag{4}$$

Flue gas sulphite and effluent metals inhibit multiplicatively, with a Hill term for sulphite and a hyperbolic term for metals,

$$f_{tox} = [1 + (C_S/K_S)^{*n^*}]^{-1} [1 + C_M/K_M]^{-1} \tag{5}$$

Nitrogen and phosphorus limitation follow Droop internal quotas, so that uptake and growth are decoupled,

$$L_N = 1 - Q_{min}/Q, \quad dQ/dt = \rho(S) - \mu Q \tag{6}$$

B. Carbonate speciation and pH-stat operation

Total alkalinity is closed over carbonate, borate and water species, and the proton concentration is obtained by geometric bisection on the residual,

$$A_T = [HCO_3^-] + 2[CO_3^{2-}] + [B(OH)_4^-] + [OH^-] - [H^+] \tag{7}$$

Dissolved inorganic carbon evolves under on-demand sparging, photosynthetic drawdown and medium exchange,

$$dC_T/dt = u\, k_L a\, (K_H\, p_{CO2} - [CO_2]) - \mu X\, f_C/M_C + D\, \Delta C_T \tag{8}$$

The valve function u(pH) opens proportionally above a setpoint of 7.85. Alkalinity is produced by nitrate assimilation at one equivalent per mole and consumed by sulphite oxidation,

$$dA_T/dt = \rho_N\, X/M_N - 2r_S + D\, \Delta A_T \tag{9}$$

C. Closed alkalinity budget and the calcification penalty

Calcification and engineered alkalinity addition compete for the same resource, so crediting them separately double-counts. Precipitating one mole of $CaCO_3$ locks one mole of carbon in the mineral but consumes two equivalents of alkalinity. Writing Y_{TA} for the alkalinity released per tonne of slag and n_{PIC} for the moles of particulate inorganic carbon formed,

$$n_{TA} = Y_{TA}\, m_{slag} - 2\, n_{PIC}$$
$$C_{carb} = \eta_{TA}\, n_{TA}\, M_C + C_{PIC} \tag{10}$$

Proposition 1. Under this budget the net durable carbon change per mole of $CaCO_3$ precipitated is $(1 - 2\eta_{TA})$, so calcification behaves as a source with an effective CO_2 release ratio

$$\psi = 2\eta_{TA} - 1 \tag{11}$$

With $\eta_{TA} = 0.79$ this gives $\psi = 0.58$, which agrees with the value of approximately 0.6 obtained independently from buffer-factor arguments for surface seawater at salinity 35. The agreement is a consistency check on the formulation rather than a new result, but it confirms that the single-budget treatment reproduces the established chemistry without assuming it.

D. Durability equivalence

Each fate pool i is characterised by a retention function giving the fraction of carbon still stored after time t,

$$R_i(t) = \exp(-t/\tau_i) \tag{12}$$

Proposition 2. Define the durability-equivalence factor as the discounted retention normalised by the discounted value of permanent storage, at social discount rate ρ. Then

$$\delta_i = \rho \int_0^\infty R_i(t)\, e^{-*\rho t*}\, dt = \rho\tau_i / (1 + \rho\tau_i) \tag{13}$$

Proof. The integral is the Laplace transform of the kernel evaluated at ρ, giving $\tau_i/(1 + \rho\tau_i)$; multiplying by ρ normalises the permanent case $\tau \to \infty$ to unity. □

The factor is strictly increasing in τ_i, tends to $\rho\tau_i$ for short-lived pools and to unity for permanent ones, and requires no arbitrary equivalence horizon. Because the transform is linear, a pool composed of sub-pools with weights w_k inherits

$$\delta = \Sigma_k\, w_k\, \rho\tau_k / (1 + \rho\tau_k) \tag{14}$$

which is used for char, modelled as 13% labile at 12 years and 87% recalcitrant at 800 years. Durability-adjusted carbon follows by weighting the partition,

$$C_{dur} = \Sigma_i\, \pi_i\, \delta_i\, C, \quad \Sigma_i\, \pi_i = 1 \tag{15}$$

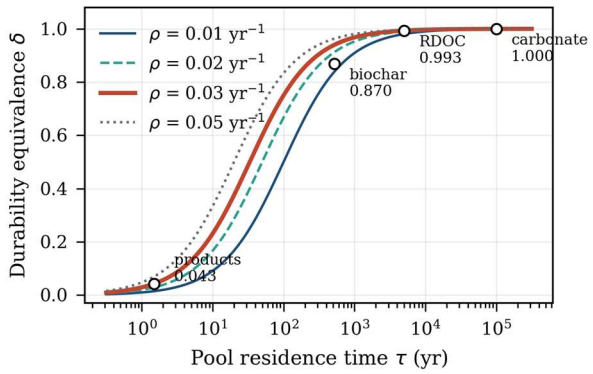

Fig. 2. Durability-equivalence factor against pool residence time. Markers give the four fate pools at $\rho = 0.03$ yr^{-1}. Short-cycle products carry a weight of 0.043, so crediting them as permanent inflates their contribution by a factor of 23.

E. Life-cycle emissions and net removal

Emissions are aggregated over electricity, thermal shortfall, slag handling, synthetic nutrient make-up, transport and amortised infrastructure,

$$E = E_{elec} + E_{th} + E_{slag} + E_{nut} + E_{tr} + E_{inf} \tag{16}$$

Nutrient make-up is charged only for demand not met by the effluent stream and internal recycling, which is the mechanism by which the circular linkage earns credit. Net durable removal, with λ the leakage fraction and ξ the CO_2-to-carbon mass ratio, is

$$C_{net} = (1 - \lambda)\, \xi\, C_{dur} - E \tag{17}$$

Proposition 3. C_{net} is affine in the grid carbon intensity I_g, since only E_{elec} and the slag milling term depend on it and both do so linearly. Hence whenever $\partial C_{net}/\partial I_g < 0$ there is a unique break-even intensity I_{crit}

$$I_{crit} = C_{net}(0) / [C_{net}(0) - C_{net}(1)] \tag{18}$$

below which the configuration is a genuine sink and above which it is a source. This is the sharpest design criterion the framework produces, because it is independent of the credit price.

F. Circularity and risk-adjusted issuance

Loop closure is summarised by the unweighted geometric mean of four normalised ratios covering durable carbon retention, nitrogen and phosphorus recovery and medium reuse,

$$BCI = (\xi_C\, \xi_N\, \xi_P\, \xi_W)^{1/4} \tag{19}$$

The geometric form is deliberate: a broken loop in any one dimension cannot be compensated by performance in the others, which an arithmetic mean would permit.

Parameter uncertainty is propagated by a scrambled Sobol' design over 20 uncertain quantities, giving a predictive distribution F for C_{net}. Credits are issued at a low quantile rather than at the mean,

$$C_{\text{iss}} = \max\{0, F^{-1}(q)\}, \quad q = 0.10 \tag{20}$$

so that the probability of over-crediting is bounded by the chosen quantile,

$$P_{\text{oc}} = \Pr(C_{\text{net}} < C_{\text{iss}}) = q \tag{21}$$

and the implied buffer pool fraction relative to mean-based issuance is

$$\beta = 1 - C_{\text{iss}} / \mathrm{E}[C_{\text{net}}] \tag{22}$$

G. Algorithm

Algorithm 1 states the full procedure. Steps 1–3 are the process model, steps 4–7 the ledger, and steps 8–10 the issuance rule.

Algorithm 1 TIDE-BC credit estimation

Input: site streams, species parameters, configuration c, discount rate ρ, quantile q
Output: issuable credits C_{iss}, buffer β
1: Integrate Eq. 1–9 over the horizon; discard start-up transient
2: Accumulate harvested carbon C_{h} and exudate C_{e} at steady state
3: Set refractory carbon $C_{\text{R}} \leftarrow \varphi_{\text{R}}\, C_{\text{e}}$
4: Resolve the alkalinity budget by Eq. 10; obtain C_{carb}
5: Partition C_{h} into product and char pools by π_{char} and char yield
6: Compute δ_{i} by Eq. 13–14 and C_{dur} by Eq. 15
7: Evaluate E by Eq. 16 and C_{net} by Eq. 17
8: **for** each Sobol' draw $\theta^{(\text{k})}$ **do** repeat steps 1–7 $\rightarrow C_{\text{net}}^{(\text{k})}$
9: Form F from $\{C_{\text{net}}^{(\text{k})}\}$; $C_{\text{iss}} \leftarrow \max\{0, F^{-1}(q)\}$
10: $\beta \leftarrow 1 - C_{\text{iss}}/\mathrm{E}[C_{\text{net}}]$; **return** C_{iss}, β

V. Simulation Setup

The coupled system is integrated with a 30-minute step over 26 days, of which the first 6 are discarded as start-up transient. Six marine species are examined: *Phaeodactylum tricornutum*, *Chaetoceros muelleri*, *Tetraselmis suecica*, *Nannochloropsis oceanica*, *Dunaliella salina* and the coccolithophore *Emiliania huxleyi*. Two thermal regimes are used, a tropical regime at 28.5/24.5 °C and a temperate regime at 21.5/17.5 °C, crossed with two silicate scenarios: effluent silicate alone at 11 mg Si L^{-1}, and ash-leachate supplementation at 88 mg Si L^{-1}.

Four process configurations form a ladder in which each step adds one circular linkage: C1 produces biomass only; C2 adds hydrothermal carbonisation; C3 adds the slag alkalinity loop; C4 substitutes low-carbon power at 0.09 kg CO_2 kWh^{-1} for grid power at 0.71 kg CO_2 kWh^{-1}. Uncertainty is propagated with 512 scrambled Sobol' draws over 20 parameters spanning physiology, site conditions and accounting coefficients.

Species kinetic parameters are nominal values selected within ranges reported for marine strains; they are not measurements and are not traceable to a single source. The model is anchored so that baseline areal productivity falls within the 15–30 g m^{-2} d^{-1} band reported for outdoor marine raceways. All results should therefore be read as relative comparisons under a stated parameterisation, not as absolute predictions for any specific site.

VI. Results and Discussion

A. Cultivation dynamics

Fig. 3 shows the reference case. Biomass rises from the inoculum to the turbidostat setpoint of 0.62 g L^{-1} by day 8, after which daily harvest removes the increment. The pH-stat holds the culture between 7.75 and 8.30 with a mean of 7.95, so the sparged CO_2 is absorbed without acidifying the pond, and dissolved CO_2 oscillates diurnally between roughly 20 and 60 µmol kg^{-1}. Nitrogen falls from 48 mg L^{-1} to below 0.3 mg L^{-1} and phosphorus is drawn down in parallel, giving steady-state polishing efficiencies of 99.5% and 97.1%. The nutrient co-benefit is therefore substantial and, notably, is not credited anywhere in the carbon ledger.

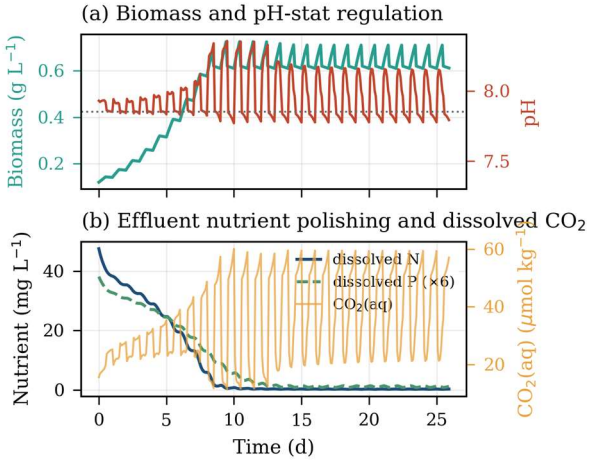

Fig. 3. Reference cultivation dynamics for *P. tricornutum* under tropical conditions with silicate supplementation. (a) Biomass and pH-stat regulation; the dotted line is the 7.85 setpoint. (b) Effluent nitrogen and phosphorus drawdown with diurnal dissolved CO_2.

B. Species screening and two negative results

Table I and Fig. 4 give the screening. Two findings run against the initial expectation.

TABLE I Species screening under tropical conditions

Species	Prod.[a]	Net, −Si[b]	Net, +Si[b]	N rem.[c]	BCI
P. tricornutum (D)	23.4	5.1	**42.8**	99.5	0.78
T. suecica	24.1	39.0	39.0	99.3	0.78
N. oceanica	17.7	36.5	36.5	98.8	0.77
C. muelleri (D)	20.0	5.7	31.2	99.5	0.77
D. salina	14.6	19.9	19.9	94.8	0.69
E. huxleyi (C)[d]	4.2	**−5.3**	**−5.3**	13.8	0.33

[a]g DW m^{-2} d^{-1}. [b]t CO_2 ha^{-1} yr^{-1}, configuration C4. [c]%. (D) diatom, (C) calcifier. [d]*E. huxleyi* values are for the temperate regime, the only one in which it grows; all other rows are tropical.

The first concerns silicate. Both diatoms collapse to zero productivity when supplied only with effluent silicate, because the demand at 0.15 g Si per g dry weight exceeds the delivery rate by roughly a factor of five. With ash-leachate supplementation *P. tricornutum* becomes the best performer at 23.4 g m^{-2} d^{-1} and 42.8 t CO_2 ha^{-1} yr^{-1}, ahead of *T. suecica* at 39.0. The diatom advantage is therefore entirely contingent on closing a second waste loop, and a project designed around diatoms without a secured silicate stream would fail outright rather than underperform. Non-siliceous species are unaffected by the scenario, which is why *T. suecica* is the robust choice where silicate supply is uncertain.

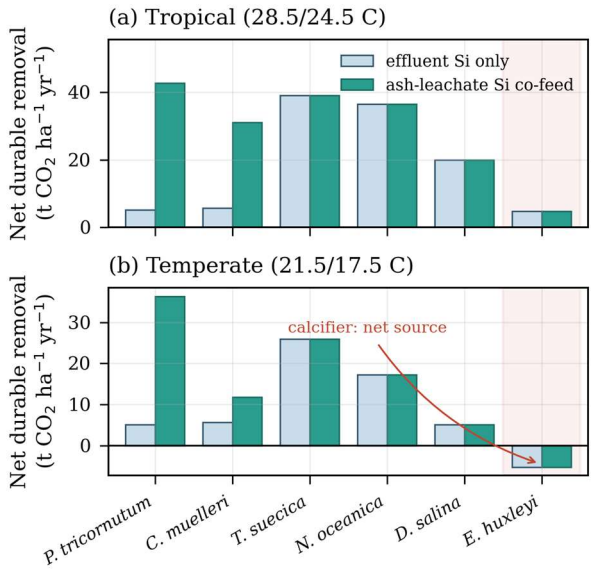

Fig. 4. Net durable removal by species under (a) tropical and (b) temperate regimes, with and without ash-leachate silicate. Shaded bands mark the calcifying species. Diatoms produce no net removal beyond the slag contribution without a silicate co-feed; the calcifier is a net source in the regime where it grows.

The second concerns calcification. *E. huxleyi* was included because coccolithophores are frequently proposed for carbon capture on the intuition that a mineral shell is durable storage. Under the closed alkalinity budget of Eq. 10 it is a net source of 5.3 t CO_2 ha^{-1} yr^{-1} in the temperate regime where it grows, because precipitating its shell forfeits more dissolved inorganic carbon storage than the shell itself contains. It does not grow at all at tropical pond temperatures. The intuitive candidate is thus doubly unsuitable, and this would have been concealed had the mineral carbon been credited separately from the alkalinity it consumed.

C. Configuration ladder

Table II and Fig. 5(a) give the ladder. Gross fixation is 213.4 t CO_2 ha^{-1} yr^{-1} in every configuration, since the cultivation stage is unchanged; what differs is where the carbon goes and what it costs to put it there.

TABLE II Configuration ladder for *P. tricornutum*

Configuration	C_{dur}[a]	E[a]	C_{net}[a]	Legacy[a]	I_{crit}[b]
C1 biomass only	12.9	145.3	−133.1	40.6	0.048
C2 + carbonisation	69.4	191.3	−125.4	−5.4	0.229
C3 + slag alkalinity	77.5	196.3	−122.6	−2.2	0.250
C4 + low-carbon power	77.5	30.8	**42.8**	163.3	0.250

[a]t CO_2 ha^{-1} yr^{-1}; gross fixation is 213.4 in all rows. [b]kg CO_2 kWh^{-1}. Legacy denotes the convention $\delta \equiv 1$ for every pool.

The durability weighting is severe. In C1, where all harvested carbon becomes short-cycle product, 213.4 t of gross fixation reduces to 12.9 t of durability-adjusted carbon, because $\delta = 0.043$ for the product pool. Adding hydrothermal carbonisation raises this to 69.4 t and adding the slag loop to 77.5 t. The pool decomposition for C4 is instructive: products carry 24.5 t C ha^{-1} yr^{-1} of raw carbon but contribute almost nothing after weighting, whereas the alkalinity pool carries only 2.2 t C but contributes essentially all of it.

More consequentially, C1 through C3 are net carbon sources, at −133.1, −125.4 and −122.6 t CO_2 ha^{-1} yr^{-1} respectively. The cause is electricity: at 0.71 kg CO_2 kWh^{-1}, cultivation and harvesting alone emit 142.6 to 185.1 t CO_2 ha^{-1} yr^{-1}. Only C4, which substitutes low-carbon power, is a sink, at 42.8 t CO_2 ha^{-1} yr^{-1}. The break-even intensity from Eq. 18 is 0.250 kg CO_2 kWh^{-1} for C3 and C4, and 0.048 for C1. This is the single most important design conclusion in the paper, and it is unfavourable to the near-term deployment case: on the present Indian grid the system cannot be creditable at any credit price.

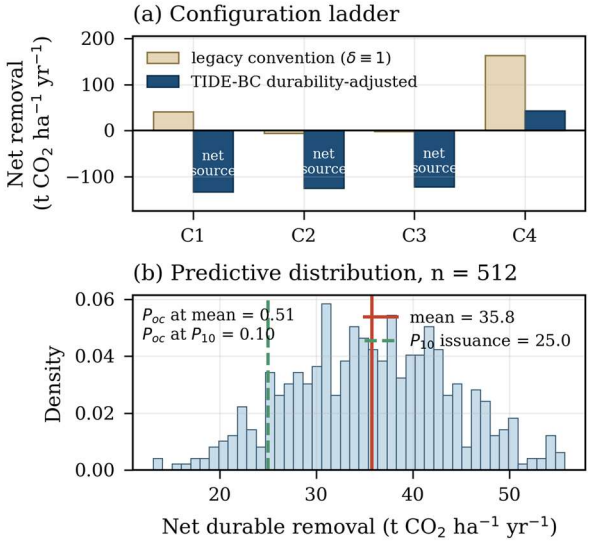

Fig. 5. (a) Configuration ladder under the legacy convention and under TIDE-BC; three of four configurations are net sources once durability weighting and life-cycle emissions are applied. (b) Predictive distribution of net removal for C4 over 512 Sobol draws, with mean and tenth-percentile issuance.

D. Uncertainty and issuance

Fig. 5(b) shows the predictive distribution for C4. The mean is 35.8 t CO_2 ha^{-1} yr^{-1} with a standard deviation of 8.3, and no draw is negative. The tenth percentile, and hence the issuable volume, is 25.0 t CO_2 ha^{-1} yr^{-1} with a bootstrap 95% interval of 23.7 to 26.1, implying a buffer fraction of 30.2%. Under the legacy convention the same draws would support a mean claim of 152.1 t, so issuing at the tenth percentile is 6.09 times more conservative than legacy mean-based issuance. For C3 every one of the 512 draws is negative, so the issuable volume is zero: the framework declines to issue rather than issuing a small positive number, which is the behaviour a regulator would want.

One result contradicts the reasoning that motivated quantile issuance. It was expected that the distribution would be strongly right-skewed, so that mean-based issuance would over-credit far more often than half the time. It is not: the distribution is close to symmetric and the over-crediting probability at the mean is 0.510, barely above the symmetric value. The case for quantile issuance therefore does not rest on skew, as originally hypothesised, but on the absolute level: a 51% chance of issuing more credits than the project delivers is an unacceptable failure rate for an environmental instrument regardless of the shape of the distribution. The hypothesis was wrong; the design conclusion survives on different grounds, and this distinction is worth stating rather than obscuring.

The sensitivity ranking in Fig. 7(a) is dominated by char yield, with a rank correlation of 0.709, followed by specific electricity demand at −0.410 and leakage at −0.285. This ordering is uncomfortable, because char yield from hydrothermal carbonisation of marine biomass is among the least well constrained parameters in the inventory. The largest lever on the result is also the one most in need of

experimental determination, and no amount of additional simulation can address that.

E. Feasibility map

Fig. 6 maps net removal over grid intensity and the fraction of carbon routed to char. The break-even contour is close to linear, and the slag loop shifts it to the right by only about 0.02 kg CO_2 kWh^{-1} — the alkalinity pathway adds durable storage but its milling and transport burden almost cancels the gain at high grid intensity. Routing more carbon to char raises the tolerable grid intensity roughly threefold across the range, from 0.05 at $\pi_{char} = 0$ to about 0.45 at $\pi_{char} = 0.85$, but even the most aggressive char routing does not reach the present grid intensity of 0.71. No combination of process choices in this design space is creditable on that grid.

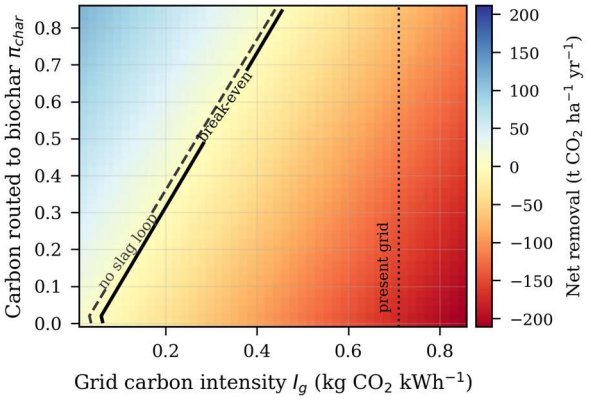

Fig. 6. Net removal over grid carbon intensity and char partition for *P. tricornutum*. Solid contour: break-even with the slag alkalinity loop; dashed: without it. The present grid intensity lies far inside the source region for all char partitions.

F. Deployment scenario and trend analysis

Fig. 7(b) projects a logistic deployment reaching 2322 ha by 2045 under two power strategies. Strategy S1 draws from the regional grid and inherits an assumed decarbonisation path from 0.71 to 0.26 kg CO_2 kWh^{-1}; strategy S2 uses co-located low-carbon generation from the outset. S1 yields no issuable credits at any point in the horizon, because the grid does not cross the break-even intensity of 0.250 until approximately 2045. S2 reaches 69.4 kt CO_2 yr^{-1} of issuable supply by 2045, against a legacy claim of 379.2 kt. Cumulatively over 2027–2045 the issuable total is 647 kt against 3535 kt claimed, a ratio of 5.46.

The policy reading is direct. Dedicated low-carbon generation is not an efficiency improvement for this class of project; it is a precondition, and a methodology that does not test for it will certify projects that increase emissions. This is a scenario under stated assumptions, not a forecast, and the adoption curve in particular is illustrative.

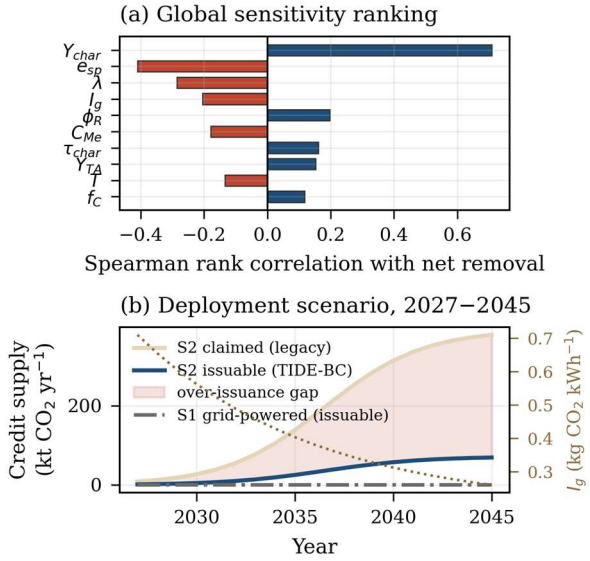

Fig. 7. (a) Global sensitivity of net removal, ranked by Spearman rank correlation over 512 Sobol draws. (b) Deployment scenario 2027–2045 comparing claimed and issuable credit supply under dedicated low-carbon power (S2), with grid-powered deployment (S1) yielding nothing throughout.

Circularity rises monotonically along the ladder, from BCI 0.322 in C1 to 0.785 in C4, driven mainly by durable carbon retention rising from 0.037 to 0.479 and medium reuse from 0.30 to 0.82. Nitrogen and phosphorus recovery are already near ceiling at 0.994 and 0.971 in every configuration, so they do not discriminate between designs; the geometric mean is nonetheless the right aggregator, because a design that lost nutrient recovery would be penalised in proportion.

VII. LIMITATIONS

The study is entirely simulation-based. No pilot, bench or field data were generated or used for validation, and no hardware was operated. The cultivation model is anchored to published productivity ranges rather than calibrated against a specific dataset, so absolute magnitudes carry more uncertainty than the Monte Carlo intervals suggest, since those intervals propagate parameter uncertainty but not structural error in the model itself.

Species kinetic parameters are nominal values within reported ranges and are not individually sourced. The relative ranking of species is more defensible than any individual figure, and even the ranking is conditional on the assumed thermal and silicate scenarios. Residence times for char and refractory dissolved organic carbon are order-of-magnitude assignments; the sensitivity analysis varies them by factors of up to two, which is likely optimistic for the refractory carbon pool in particular.

Several real effects are absent. Culture crashes, grazer and viral contamination, and seasonal variation are not modelled, and a 26-day integration cannot capture them; the annualisation from a steady-state window to a yearly rate assumes uninterrupted operation and is therefore an upper bound. Trace metal speciation is treated as a single lumped concentration. Slag alkalinity release is modelled as a fixed yield rather than a dissolution kinetic, and the fate of metals leached from slag is not tracked, which is a genuine environmental risk that this analysis does not quantify. The avoided emissions from wastewater treatment that the system displaces are deliberately not credited, which makes the results conservative in that one respect.

Finally, the framework prices durability but not permanence risk from reversal events such as char combustion or land-use change, which would require a hazard model rather than a retention kernel.

VIII. Conclusion

Durability weighting changes blue carbon crediting from an accounting formality into a binding design constraint. Deriving the equivalence factor as $\delta = \rho\tau/(1 + \rho\tau)$ removes the need for an arbitrary equivalence horizon and shows immediately that short-cycle biomass products, at $\delta = 0.043$, cannot support credit revenue whatever their market value as products. Resolving calcification and engineered alkalinity on one closed budget removes a double-counting error and reproduces the surface-seawater CO_2 release ratio as a derived quantity.

Applied to a coastal industrial symbiosis loop, the framework identifies *P. tricornutum* with ash-leachate silicate as the best of six candidates at 42.8 t CO_2 ha^{-1} yr^{-1}, with a risk-adjusted issuance of 25.0 t CO_2 ha^{-1} yr^{-1} and a 30.2% buffer. It also returns three findings that a proponent would prefer not to publish: three of four configurations are net sources on the present grid, the diatoms fail entirely without a second waste loop, and the coccolithophore is a net source. The break-even grid intensity of 0.250 kg CO_2 kWh^{-1} is the operative screening criterion, and any methodology for this project class that does not test it will certify emitters as removers.

Experimental determination of hydrothermal char yield and its residence-time distribution for marine biomass is the highest-value next step, since that parameter dominates the sensitivity ranking and is the least constrained. Pilot validation of the coupled pH-stat and alkalinity budget under real flue gas is the necessary second.

IX. Acknowledgment

The authors thank colleagues at the Research and Development Division, Tekstein Solutions Private Limited, for discussion of the accounting framework. No external funding was received for this work.

. References

[1] R. A. Houghton, "Balancing the global carbon budget," Annu. Rev. Earth Planet. Sci., vol. 35, pp. 313–347, 2007.

[2] C. Nellemann, E. Corcoran, C. M. Duarte, L. Valdes, C. De Young, L. Fonseca, and G. Grimsditch, Blue Carbon: The Role of Healthy Oceans in Binding Carbon. Arendal, Norway: UNEP/GRID-Arendal, 2009.

[3] J. B. Smith, S. Brown, and W. R. Moomaw, "Ton-year accounting for temporary carbon storage," Climatic Change, vol. 89, pp. 205–222, 2008.

[4] K. Dooley and S. Kartha, "Land-based negative emissions: risks for climate mitigation and equity," Int. Environ. Agreements, vol. 18, pp. 79–98, 2018.

[5] N. Jiao, G. J. Herndl, D. A. Hansell, R. Benner, G. Kattner, S. W. Wilhelm, D. L. Kirchman, M. G. Weinbauer, T. Luo, F. Chen, and F. Azam, "Microbial production of recalcitrant dissolved organic matter," Nature Rev. Microbiol., vol. 8, pp. 593–599, 2010.

[6] P. Renforth and G. Henderson, "Assessing ocean alkalinity for carbon sequestration," Rev. Geophys., vol. 55, pp. 636–674, 2017.

[7] A. F. Dickson, C. L. Sabine, and J. R. Christian, Eds., Guide to Best Practices for Ocean CO2 Measurements. Sidney, BC: PICES Special Publication 3, 2007.

[8] L. Rosso, J. R. Lobry, and J. P. Flandrois, "An unexpected correlation between cardinal temperatures of microbial growth highlighted by a new model," J. Theor. Biol., vol. 162, pp. 447–463, 1993.

[9] S. Aiba, "Growth kinetics of photosynthetic microorganisms," Adv. Biochem. Eng., vol. 23, pp. 85–156, 1982.

[10] M. R. Droop, "Some thoughts on nutrient limitation in algae," J. Phycol., vol. 9, pp. 264–272, 1973.

[11] M. A. Brzezinski, "The Si:C:N ratio of marine diatoms: interspecific variability and the effect of some environmental variables," J. Phycol., vol. 21, pp. 347–357, 1985.

[12] U. Riebesell, I. Zondervan, B. Rost, P. D. Tortell, R. E. Zeebe, and F. M. M. Morel, "Reduced calcification of marine plankton in response to increased atmospheric CO2," Nature, vol. 407, pp. 364–367, 2000.

[13] E. Stephens, I. L. Ross, Z. King, J. H. Mussgnug, O. Kruse, C. Posten, M. A. Borowitzka, and B. Hankamer, "An economic and technical evaluation of microalgal biofuels," Nature Biotechnol., vol. 28, pp. 126–128, 2010.

[14] A. F. Clarens, E. P. Resurreccion, M. A. White, and L. M. Colosi, "Environmental life cycle comparison of algae to other bioenergy feedstocks," Environ. Sci. Technol., vol. 44, pp. 1813–1819, 2010.

[15] J. A. Libra, K. S. Ro, C. Kammann, A. Funke, N. D. Berge, Y. Neubauer, M. M. Titirici, C. Fühner, O. Bens, J. Kern, and K. H. Emmerich, "Hydrothermal carbonization of biomass residuals," Biofuels, vol. 2, pp. 71–106, 2011.

[16] J. Lehmann, S. Abiven, M. Kleber, G. Pan, B. P. Singh, S. Sohi, and A. Zimmerman, "Persistence of biochar in soil," in Biochar for Environmental Management, 2nd ed., London: Routledge, 2015, pp. 235–282.

[17] W. Wang, C. Xu, J. Jin, and Y. Zhang, "Steel slag as a carbon sink and alkalinity source: a review," J. Cleaner Prod., vol. 282, art. 124532, 2021.

[18] K. Kumar, C. N. Dasgupta, B. Nayak, P. Lindblad, and D. Das, "Development of suitable photobioreactors for CO2 sequestration addressing global warming," Bioresour. Technol., vol. 102, pp. 4945–4953, 2011.

[19] N. Abdel-Raouf, A. A. Al-Homaidan, and I. B. M. Ibraheem, "Microalgae and wastewater treatment," Saudi J. Biol. Sci., vol. 19, pp. 257–275, 2012.

[20] I. M. Sobol', "Global sensitivity indices for nonlinear mathematical models and their Monte Carlo estimates," Math. Comput. Simulation, vol. 55, pp. 271–280, 2001.

[21] B. K. Haya, S. Evans, L. Brown, J. Bukoski, V. Butsic, B. Cabiyo, R. Jacobson, A. Kerr, M. Potts, and D. L. Sanchez, "Comprehensive review of carbon quantification by improved forest management offset protocols," Front. For. Glob. Change, vol. 6, art. 958879, 2023.

[22] Central Electricity Authority, CO2 Baseline Database for the Indian Power Sector, User Guide Version 19. New Delhi, India: Ministry of Power, Government of India, 2023.